Investigating negative capacitance shunt circuit for broadband vibration damping and utilizing ACO for optimization

AZNI N WAHID [1], ASAN G A MUTHALIF [2], KHAIRUL A M NOR
Smart Structures, Systems & Control Research Laboratory (S^3CRL)
Department of Mechatronics Engineering,
International Islamic University Malaysia
Jalan Gombak, 53100 Kuala Lumpur
MALAYSIA
[1] azni.nabela.wahid@gmail.com, [2] asan@iium.edu.my

Abstract: - This paper presents optimization of vibration damping for a rectangular thin plate using a single piezoelectric (PZT) patch shunted with negative capacitance, by utilizing the ant colony optimization (ACO) algorithm. The frequency range to be controlled is presented in the context of statistical energy analysis (SEA) where modal overlap factor (MOF) is considered i.e. MOF<1 (low), 1<MOF<2 (mid) and MOF>2 (high). The effects of two different shunt circuits on the system are studied; series and parallel resistor-negative capacitor (R-C). The governing equation of motion for a PZT patch shunt attached on a thin plate is obtained using Lagrange's equation, and ACO algorithm is utilized to obtain the optimum spatial coordinate of the PZT patch and resistor values of the shunt circuit for the different frequency regions, targeting for maximum energy reduction of the vibrating thin plate.

Key-words: - Piezoelectric shunt damping, Negative capacitance, Statistical Energy Analysis, modal overlap factor, Ant Colony Optimization.

1 Introduction

Connecting the terminals of a PZT transducer to an external electrical circuit is called shunting, which capable of extracting vibration energy from the host structure and dissipate the energy through Joule heat i.e. provide damping to the system. The most attractive attribute of negative capacitance shunting aside from its simplicity is that it is independent of the structural resonance frequencies [1]. The negative capacitance by itself does not dissipate energy; however it does help to enhance the dissipation of energy in the passive circuit by improving the conversion of energy in the transducer. This is done by cancelling out or reducing the inherent capacitance of the PZT [2].

Work by [1] has shown that the negative capacitance controller is capable of damping modally dense thin plate, i.e.4^{th} and 5^{th} modes and is insensitive to the environmental conditions. They proved this by shifting the resonance by 2% of its original, in which the performance did not significantly deteriorate. [3] in their work has shown theoretically that a series R-C circuit is capable of suppressing the vibration amplitudes in lower frequency range, while the one connected to parallel R-C is capable of suppressing vibration amplitude in high frequency range, using the same resistor value. Beck et al. in [4] showed that it is possible to obtain the same frequency behaviour using either series or parallel R-C configuration, by using significantly different resistor values. Therefore, there may be no advantage of using either configuration for negative shunting. While a lot of research work done in negative capacitance shunting emphasized on its capability to suppress vibration in wide frequency range, it is found that no research has yet specify the range of frequency to be controlled in line with SEA context i.e. how high is high frequency and how to determine it.

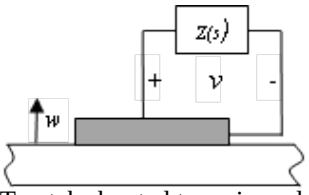

Fig.1: PZT patch shunted to an impedance Z(s)

The term 'high' in 'high-frequency vibration' context is not simply numerical. High-frequency implies that the frequency range extends to many times the fundamental natural frequency of a structure under consideration. Statistical modelling method such as Statistical Energy Analysis (SEA) is commonly employed for analyzing high-frequency vibration in engineering structures. Unlike classical vibration analysis which is based on force and displacement, SEA approach uses energy quantities such as energy, energy density and power. The main aim of the SEA method is to predict energy distribution among subsystems. One of the parameters used in SEA is modal overlap factor (MOF). MOF is used to quantify the degree of overlap in modal response i.e. the ratio of the half-power bandwidth to the local average interval between natural frequencies [5, 6].

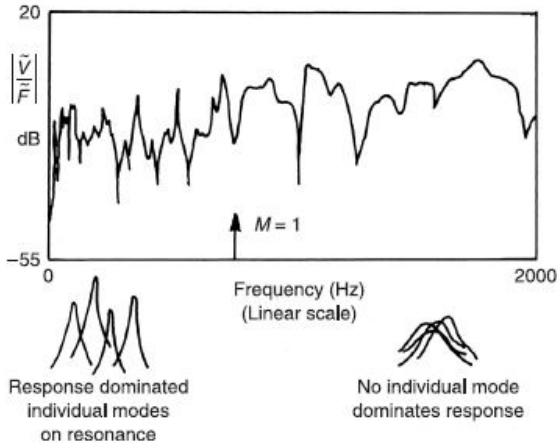

Fig. 2: Frequency response function of a rectangular plate to show MOF [5]

$$MOF(\omega) = n\omega\eta = \frac{A}{4\pi}\sqrt{\frac{\rho h}{D}}\omega\eta \quad (1)$$

Where n is the modal density, η is the modal loss factor, ω frequency in rad/s, A is the surface area of the structure ρ, h and D are the density, thickness and the flexural rigidity of the structure, respectively. At low frequency range, where MOF<1, individual modal responses are distinctly visible. As MOF≈1, the individual modal responses begin to overlap and as MOF>1, no distinct resonant peaks are visible in the response. This brings problem for modal-based vibration control where modal amplitude suppression is employed [5].

This paper will simulate broadband control (in SEA context) using a single PZT patch shunted with R-C circuit using series and parallel circuit configuration in three frequency regions i.e. MOF<1, 1<MOF<2 and MOF>2. Parameter optimization will be conducted using ant colony optimization (ACO) technique. Muthalif et al. in [7] showed that the PZT patch location is not important at high frequency, thus, the optimal patch placement will be done only for MOF<1 and used for the other frequency regions.

2 Modelling of a thin plate attached with a shunted PZT patch

The PZT constitutive equation is introduced as:

$$\begin{bmatrix}\sigma\\ z\end{bmatrix} = \begin{bmatrix}c^E & -e^t\\ e & \varepsilon^S\end{bmatrix}\begin{bmatrix}S\\ E\end{bmatrix} \quad (2)$$

Where $\boldsymbol{c}$ is the modulus of elasticity, e is the piezoelectric coupling coefficient and relates the stress to the applied electrical field, and ε is the dielectric matrix. The superscript E and S indicates that the parameter was measured at constant electric field (short circuit) and strain, respectively. Hagood and Von Flotow [8] showed how to use Eq. (2) to obtain the general equation for a PZT in terms of the external current input and applied voltage:

$$\begin{bmatrix}I\\ \sigma\end{bmatrix} = \begin{bmatrix}Y^{EL} & sAe\\ -e^t t_p^{-1} & c^E\end{bmatrix}\begin{bmatrix}V\\ S\end{bmatrix}, \quad (3)$$

$$Y^{EL} = Y^D_{PZT} + Y^{shunt} \quad \text{and} \quad Z = 1/Y \quad (4)$$

Where I is the electric current, V is the electric voltage, A is the surface area perpendicular to the electrical field (diagonal matrix), t_p is the thickness

of the patch, Y is the electrical admittance and $Y_{PZT}^{D} = sC_{pzt}^{s}$. The stress expression is updated as:

$$\mathrm{c}^{\mathrm{shunt}} = [\mathrm{c}^{\mathrm{E}} + \mathrm{e}^{\mathrm{t}}\bar{\mathrm{Z}}^{\mathrm{EL}}(\varepsilon^{\mathrm{S}})^{-1}\mathrm{e}] \quad (5)$$

And the new modulus of elasticity for a shunted PZT is defined as:

$$\sigma = [\mathrm{c}^{\mathrm{E}} + \mathrm{e}^{\mathrm{t}}\bar{\mathrm{Z}}^{\mathrm{EL}}(\varepsilon^{\mathrm{S}})^{-1}\mathrm{e}]\mathrm{S} - [\mathrm{e}^{\mathrm{t}}\mathrm{t}_{\mathrm{p}}^{-1}\mathrm{Z}^{\mathrm{EL}}]\mathrm{I} \quad (6)$$

Where the matrix of non-dimensional electrical impedance is:

$$\bar{\mathrm{Z}}^{\mathrm{EL}} = \mathrm{Z}^{\mathrm{EL}}\left(\mathrm{Z}_{\mathrm{PZT}}^{\mathrm{D}}\right)^{-1} = \left(\mathrm{sC}_{\mathrm{pzt}}^{\mathrm{s}} + \mathrm{Y}^{\mathrm{shunt}}\right)^{-1}\mathrm{sC}_{\mathrm{pzt}}^{\mathrm{s}} \quad (7)$$

$$\bar{Z}^{EL} = 1, \text{for open circuit}$$

To obtain the total equation of motion for the thin plate attached with a shunted PZT patch, Lagrange equation is employed:

$$\frac{\partial}{\partial \mathrm{t}}\left(\frac{\partial \mathrm{L}}{\partial \dot{\mathrm{q}}_{\mathrm{r}}}\right) - \frac{\partial \mathrm{L}}{\partial \mathrm{q}_{\mathrm{r}}} = \mathrm{Q}_{\mathrm{r}}\ ;\ \text{where L} = \mathrm{T} - \mathrm{U} \quad (8)$$

Where q_r is the generalized coordinate of the system and $Q_r = \frac{\delta W}{\delta q_r}$ is the generalized force, T and U are the total kinetic and potential energies of the system, respectively which defined as:

$$\mathrm{T} = \frac{1}{2}\rho_{st}\int_{\mathrm{V_{st}}} \dot{\mathrm{w}}^{\mathrm{t}}\dot{\mathrm{w}}\,\mathrm{dV_{st}} + \frac{1}{2}\rho_{\mathrm{pz}}\int_{\mathrm{V_{pzt}}} \dot{\mathrm{w}}^{\mathrm{t}}\dot{\mathrm{w}}\,\mathrm{dV_{pzt}} \quad (9)$$

$$\mathrm{U} = \frac{1}{2}\int_{\mathrm{V_{st}}} \mathrm{S}^{\mathrm{t}}\sigma_{\mathrm{st}}\,\mathrm{dV_{st}} + \frac{1}{2}\int_{\mathrm{V_{pzt}}} \mathrm{S}^{\mathrm{t}}\sigma_{\mathrm{pzt}}\,\mathrm{dV_{pzt}}, \quad (10)$$

$$\delta\mathrm{W} = \sum_{\mathrm{i}=1}^{\mathrm{nf}} \delta\mathrm{w}(\mathrm{x_i}, \mathrm{y_i}).\,\mathrm{f_i}(\mathrm{x_i}, \mathrm{y_i}) \quad (11)$$

Where δW is the external work applied to the system, V is the volume, w is the transverse displacement, subscript *st* and *pzt* represent host structure and PZT material respectively. σ_{pzt} is Eq. (5). Since a simply-supported plate is used, the deflection of the plate during vibration can be assumed as the double series:

$$w(x, y, t) = \sum_{m}\sum_{n} W_{mn}(t)\, sin\frac{m\pi x}{a} sin\frac{n\pi y}{b} \quad (12)$$

Therefore,

$$-\omega^2[\mathrm{M}]\{\mathrm{W_{mn}}\} + [\mathrm{K_C}]\{\mathrm{W_{mn}}\} + [\theta]\,\bar{\mathrm{Z}}^{\mathrm{EL}}\left(\varepsilon^{\mathrm{S}}\right)^{-1}\{\mathrm{W_{mn}}\} = \{\mathrm{F_{mn}}\} \quad (13)$$

$$\{\mathrm{W_{mn}}\} = (-\omega^2[\mathrm{M}] + [\mathrm{K_C}] + [\theta]\,\bar{\mathrm{Z}}^{\mathrm{EL}}\left(\varepsilon^{\mathrm{S}}\right)^{-1})^{-1}\{\mathrm{F_{mn}}\} \quad (14)$$

$$\mathrm{EP}(\omega) = \frac{1}{2}\mathrm{W_{mn}}^{\mathrm{T}}[\mathrm{K_C}]\mathrm{W_{mn}} \quad (15)$$

Where [M], [K_C], and [θ] represent total modal mass, total complex modal stiffness, and modal electromechanical coupling, respectively, $\{W_{mn}\}$ and $\{F_{mn}\}$ are the modal coordinate vector and applied mechanical force vector, respectively. [K_C] is used to account for structural loss where [K_C] = [K](1+jη); η is modal loss factor and EP(ω) is the energy of the system.

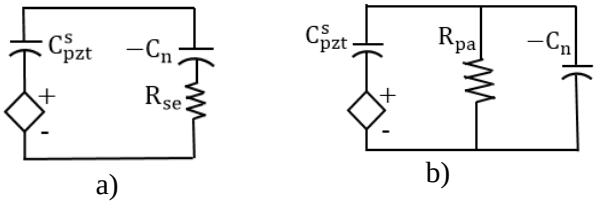

Fig. 3: Circuit model of piezoelectric shunted with a) series b) parallel resistor-negative capacitor (R-C) circuit

In this study, two different R-C circuit configurations will be used for shunting. An analysis of the circuits in Fig. 3 leads to the expressions in (16-19), (subscript *se* and *pa* for series and parallel respectively). Condition $C_n > C_{pzt}^{s}$ is met to ensure stability [9].

$$\mathrm{Y_{se}}(\mathrm{s}) = \frac{1}{\mathrm{R_{se}} - \frac{1}{\mathrm{sC_n}}}, \quad (16)$$

$$\bar{Z}_{se}^{EL}(s) = \frac{C_{pzt}^{s}(sR_{se}C_n - 1)}{C_{pzt}^{s}(sR_{se}C_n - 1) + C_n} \quad (17)$$

$$Y_{pa}(s) = \frac{1}{R_{pa}} - sC_n, \quad (18)$$

$$\bar{Z}_{pa}^{EL}(s) = \frac{sR_{pa}C_{pzt}^{s}}{sR_{pa}(C_{pzt}^{s} - C_n) + 1} \quad (19)$$

3 ACO for optimization

ACO algorithm is inspired by the behaviour of real ants in which the ants uses pheromones as a communication medium in finding food source [10]. Global cooperation among ants in a colony can produce promising paths towards the food source. An ant deposits pheromone trails on the ground while looking for the food. The next ants will tend to follow the stronger trails and also reinforcing the trail with their own pheromone, which consequently making the path more favourable as compared to others. Meanwhile, the weaker trails progressively decreased by evaporation.

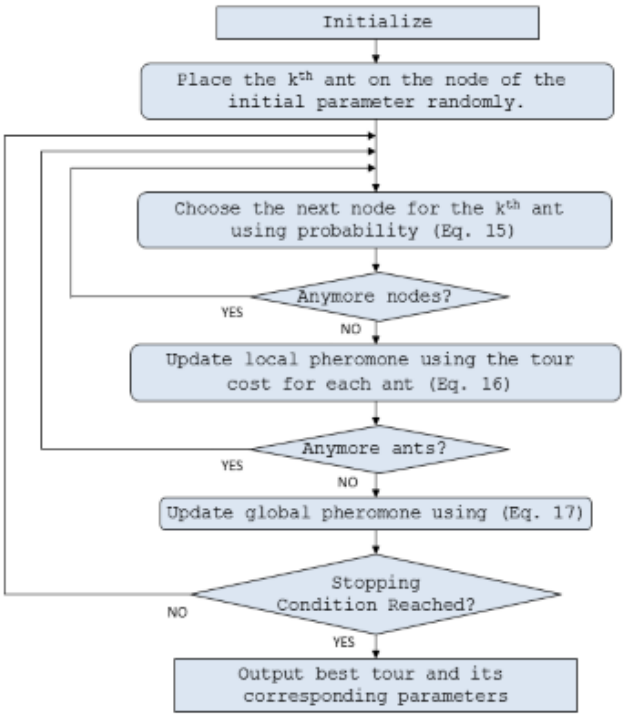

Fig. 4: Flowchart of SACO

Simple-ACO (SACO), a variation of ACO, is employed in this paper. SACO algorithm is basically similar to Ant System algorithm, but without heuristic value and it was successfully used for optimization problems [11, 12] . The probability equation in SACO can be written as:

$$P_k(t) = \begin{cases} \frac{\{\tau_{ij}(t)\}^{\alpha}}{\sum_{i,j\in T_k}\{\tau_{ij}(t)\}^{\alpha}} & , \text{if } j \in T_k \\ 0 & , \text{otherwise} \end{cases} \quad (20)$$

where τ is the pheromone trail, t is time, α is the constant that defines the relative importance of the pheromone values and T_k is the path effectuated by the ant k at a given time. The value of tour taken by each ant is:

$$\Delta\tau_{ij}(t) = \begin{cases} \frac{Q}{L_k} & , \text{if } (i,j) \text{walked by ant k.} \\ 0 & , \text{otherwise} \end{cases} \quad (21)$$

where Q is a contant and L_k is the cost of tour by ant k or the objective function. In this paper, L_k is the inverse of energy reduction calculated using Eq. (18). After each ant performs a complete tour, the pheromone trails are updated using:

$$\tau_{ij}(t) = \sigma\tau_{ij}(t-1) + \sum_{k=1}^{NA}\Delta\tau_{ij}(t) \quad (22)$$

where σ is the pheromone decay $0 < \sigma < 1$ to introduce the forgetfulness of the bad choices and NA is the number of ants. In this study, NA=20, maximum generation is 50, α=1 and $\sigma = 0.75$ are used. The flowchart of the SACO algorithm is shown in Fig. 4.

The objective function of the system is defined in eqn. (23), where $\overline{EP_c}$ and $\overline{EP_{nc}}$ are the average plate energy with and without control, respectively. The frequency range of interest is divided into three regions; MOF<1 at 1-367Hz, 1<MOF<2 at 367-735Hz and MOF>2 at >735Hz.

$$\text{minimize } \frac{1}{ER} = \frac{\overline{EP_{nc}}}{\overline{EP_{nc}} - \overline{EP_c}} \quad (23)$$

4 Simulation results

For simulation studies, a stainless steel rectangular thin plate with dimension (0.7x0.6x0.001m) is used, excited by an arbitrary point force and controlled using a single shunted piezoelectric patch (PZT-5A). Two cases will be studied i.e. when the patch is shunted with a series and a parallel R-C circuit, respectively. The location of the patch and the resistor values, Rse and Rpe are the variables to be optimized. According to [9], a negative capacitance 2-5% greater than the PZT capacitance will provide good damping performance with acceptable robustness to small changes in environmental temperature. From the optimization, it is found out that the optimized location for both series and parallel configurations are about the same. Thus, the simulation is carried out to find the optimized resistance, *R* only. The following table summarized the result for optimization performed via ACO:

Table 1: ACO simulation results

	Series	**Parallel**
MOF< 1	*R* = 611 Ω	*R* = 2.5816e6 Ω
1<MOF< 2	*R* = 110 Ω	*R* = 6.4403e5 Ω
MOF > 2	*R* = 90 Ω	*R* = 2.8951e5 Ω
Patch location on plate: (0.155m, 0.194m) from plate corner		

The poor control performance associated with the first mode is due to the placement of the patch, which is found by optimizing the *average of total* energy reduction at a broad frequency range. Interesting observation can be made for MOF>1 (Figs. 5b&c). The controlled responses are about the same for both series and parallel configurations with very small difference in average energy reduction. This is seemingly the maximum average energy reduction achievable for this particular patch placement. On the other hand, at low frequency range (MOF<1, Fig. 5a), the difference of performance can be recognized where the average energy reduction achieved by the optimized series circuit is about 7% lesser than the optimized parallel circuit.

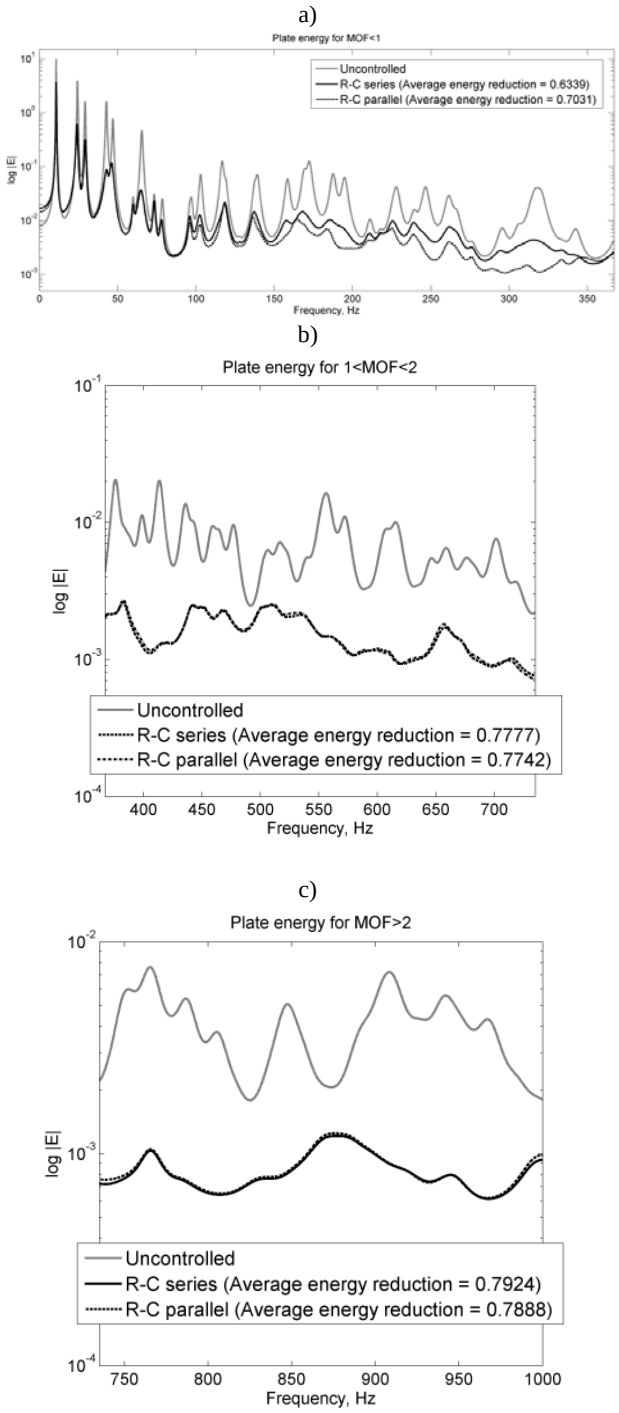

Fig. 5: Comparison of plate energy between open circuit and with shunted PZT patch in series and parallel configurations at a) MOF<1, b) 1<MOF<2, c) MOF>2

5 Conclusions

From the simulation results, it can be deduced that it is possible to obtain the same frequency behaviour

using either series or parallel R-C configuration, by using significantly different resistor values for response at MOF>1.Therefore, there may be no advantage of using either configuration for negative shunting at this range, except for physical implementation where parallel configuration requires significantly high resistance value. From the studies, negative capacitance shunt damping is proven suitable for broadband vibration control i.e. modally dense vibration response (MOF>1) which exhibits no distinct modes.

Acknowledgements

This work was supported by Fundamental Research Grant Scheme (FRGS15-165-0406) from the Ministry of Higher Education Malaysia.

References:

[1] S. Behrens, A. Fleming, and S. Moheimani, "A broadband controller for shunt piezoelectric damping of structural vibration," *Smart Materials and Structures,* vol. 12, p. 18, 2003.

[2] B. De Marneffe and A. Preumont, "Vibration damping with negative capacitance shunts: theory and experiment," *Smart Materials and Structures,* vol. 17, p. 035015, 2008.

[3] C. H. Park and H. C. Park, "Multiple-mode structural vibration control using negative capacitive shunt damping," *KSME international journal,* vol. 17, pp. 1650-1658, 2003.

[4] B. S. Beck, K. A. Cunefare, and M. Collet, "The power output and efficiency of a negative capacitance shunt for vibration control of a flexural system," *Smart Materials and Structures,* vol. 22, p. 065009, 2013.

[5] F. J. Fahy and P. Gardonio, *Sound and structural vibration: radiation, transmission and response*: Academic press, 2007.

[6] R. S. Langley and A. N. Bercin, "Wave intensity analysis of high frequency vibrations," *Philosophical Transactions of the Royal Society of London. Series A: Physical and Engineering Sciences,* vol. 346, pp. 489-499, 1994.

[7] A. G. A. Muthalif, A. N. Wahid, and K. A. M. Nor, "Estimating ensemble average power delivered by a piezoelectric patch actuator to a non-deterministic subsystem," *Journal of Sound and Vibration,* vol. 333, pp. 1149-1162, 2014.

[8] N. W. Hagood and A. von Flotow, "Damping of structural vibrations with piezoelectric materials and passive electrical networks," *Journal of Sound and Vibration,* vol. 146, pp. 243-268, 1991.

[9] S. R. Moheimani and A. J. Fleming, *Piezoelectric transducers for vibration control and damping*: Springer, 2006.

[10] M. Dorigo and T. Stützle, *Ant Colony Optimization*: MIT Press, Bradford Books, 2004.

[11] M. Dorigo and T. Stützle, "An Experimental Study of the Simple Ant Colony Optimization Algorithm," 2001.

[12] M. Garcia, O. Montiel, O. Castillo, R. Sepúlveda, and P. Melin, "Path planning for autonomous mobile robot navigation with ant colony optimization and fuzzy cost function evaluation," *Applied Soft Computing,* vol. 9, pp. 1102-1110, 2009.